Analytica Chimica Acta 1335 (2025) 343450

Contents lists available at ScienceDirect

Analytica Chimica Acta

journal homepage: www.elsevier.com/locate/aca

Sequencing the monoclonal antibody variable regions using multiple charge integration middle-down strategy and ultraviolet photodissociation

Jialiang Liu [a,b,c], Zheyi Liu [b,c,d,**], Heng Zhao [b,c], Chunlei Xiao [c,d], Xueming Yang [c], Fangjun Wang [b,c,d,*]

[a] School of Pharmacy, China Medical University, Shenyang, 110122, China
[b] CAS Key Laboratory of Separation Sciences for Analytical Chemistry, Dalian Institute of Chemical Physics, Chinese Academy of Sciences, Dalian, 116023, China
[c] State Key Laboratory of Molecular Reaction Dynamics, Dalian Institute of Chemical Physics, Chinese Academy of Sciences, Dalian, 116023, China
[d] University of Chinese Academy of Sciences, Beijing, 100049, China

HIGHLIGHTS

- The MCI strategy achieved over 95 % sequence coverage of mAbs.
- Successfully achieved full sequence coverage of CDRs.
- Multiple PTMs of mAb were accurately identified, including glycosylation, lysine truncation, and glutamine cyclization.

GRAPHICAL ABSTRACT

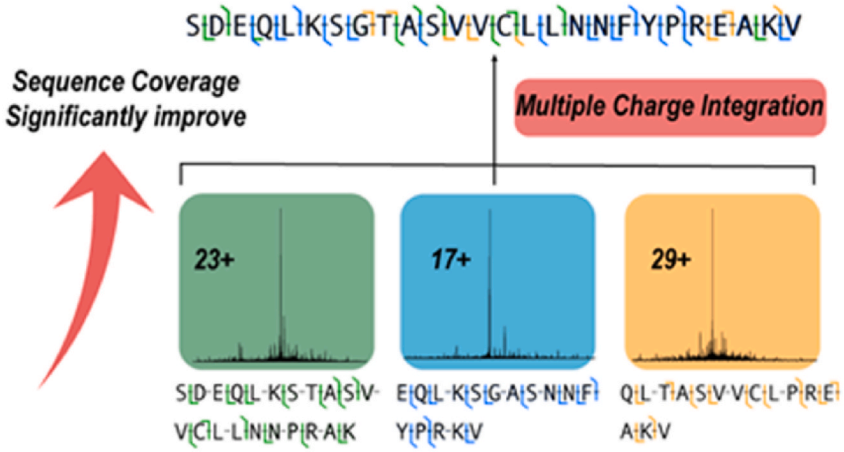

ARTICLE INFO

Handling Editor: Dr. L. Liang

Keywords:
mAb
UVPD
Middle-down

ABSTRACT

Background: Therapeutic monoclonal antibodies (mAbs) have become essential biopharmaceuticals for clinical targeted therapies due to their high specificity, affinity and low side effects. The specificity and affinity of mAb to targeting antigen are mainly dependent on the three complementarity determining regions (CDRs) with high variations in amino acid sequences. Therefore, mAb CDR sequencing is crucial for the characterization of therapeutic mAbs. Here, we developed a 193-nm ultraviolet photodissociation (UVPD) based multiple charge integration middle-down mass spectrometry (MCI-MDMS) strategy for mAb sequencing.

* Corresponding author. CAS Key Laboratory of Separation Sciences for Analytical Chemistry, Dalian Institute of Chemical Physics, Chinese Academy of Sciences, Dalian, 116023, China.
** Corresponding author. CAS Key Laboratory of Separation Sciences for Analytical Chemistry, Dalian Institute of Chemical Physics, Chinese Academy of Sciences, Dalian, 116023, China.
E-mail addresses: zy_liu@dicp.ac.cn (Z. Liu), wangfj@dicp.ac.cn (F. Wang).

https://doi.org/10.1016/j.aca.2024.343450
Received 9 August 2024; Received in revised form 15 November 2024; Accepted 19 November 2024
Available online 19 November 2024

MCI
CDR sequencing

Results: We demonstrate that the UVPD spectra of mAb subunit ions with different charge states exhibit high complementarity, and integration can result in higher sequence coverage compared to single charge states. Finally, over 95 % sequence coverage of two different mAbs has been achieved with full sequence coverage of CDRs, underscoring the great potential of this strategy in accurate sequencing of mAb variable regions. Compared with the conventional higher energy collisional dissociation (HCD) strategy of mAb subunit sequencing, the sequence coverage of CDRs at single UVPD subunit charge state has increased by an average of 30 %. In addition, almost complete sequence coverage of mAb ensures the accurate localization of mAb post-translational modifications (PTMs), including glycosylation of two different sites, C-terminal lysine truncation, and N-terminal cyclization of glutamine.
Significance: The integration of MCI-MDMS and UVPD realizes high sequence coverage and reliable PTM determination of mAbs. This integrated strategy holds significant promise for accurate analysis of antibody-drug conjugates, polyclonal antibodies and unknown mAbs including sequences and PTMs, and providing a crucial tool for the discovery and development of therapeutic mAbs.

1. Introduction

Monoclonal antibodies (mAbs) have emerged as powerful targeted biopharmaceuticals in the clinical cancer treatment [1,2]. Since the first mAb drug was approved by FDA in 1986, therapeutic mAbs account for one-fifth of FDA new drug approvals, with over 100 mAb drugs approved by 2021 [3,4]. The great success of mAb drugs is mainly attribute to their high specificity to protein targets, high affinity, and low side effects, exhibiting great potential in the treatment of cancer, autoimmune disease, and viral infections [5–8]. While the majority of currently approved therapeutic mAbs belong to immunoglobulin G (IgG), composed of two heavy chains (HC) (~50 kDa) and two light chains (LC) (~25 kDa) [9], the field is rapidly expanding to include other antibody formats. Humanized antibodies, engineered to minimize immunogenicity in humans, are enhancing therapeutic efficacy and safety. Bispecific antibodies target two different antigens simultaneously, potentially enhancing treatment efficacy and overcoming tumor resistance mechanisms [10]. Antibody-drug conjugates (ADCs) link a cytotoxic drug to an antibody, delivering the payload specifically to cancer cells while minimizing damage to healthy tissues [11]. The N-terminal parts of HC (~50 kDa) and LC (~25 kDa) are the complementarity determining regions (CDRs) with highly variable site sequences, which are used for the specific target binding [12,13]. There are three CDRs in these variable regions, determining the specificity and diversity of antibody-target recognition and binding [14–16]. Therefore, mAb sequencing, especially CDR sequence determination, is crucial for developing and ensuring the quality control of therapeutic mAbs across all formats.

Tandem mass spectrometry (MS/MS) is emerging as a powerful tool for antibody sequencing, commonly using bottom-up MS (BUMS) strategy for proteolytic peptide analysis [15,17,18]. The digestion of mAb into peptides facilitates the fragmentation by MS/MS, but loss the connectivity of mAb functional sequences especially CDRs. Moreover, the multi-step and tedious sample preparation procedures of BUMS analysis tend to introduce artificial interferences. Top-down MS (TDMS) strategy can analyze the mAb sequence directly without any sample preparation. However, the large size and disulfide bonds of mAbs greatly challenge the current MS fragmentation methods, commonly resulting in low sequence coverages [19,20]. A compromise approach is the middle-down MS (MDMS) strategy by pre-cleavage of IgG into three subunits Fc/2, Fd, and Lc with molecular weights (MWs) about 25 kDa by *Streptococcus pyogenes* (IdeS) [9,21–23]. Fornelli et al. applied MDMS strategy to sequence the IdeS pre-cleaved adalimumab by integrating 3000 electron-transfer dissociation (ETD) MS/MS spectra, and 68.5 % sequence coverage was obtained for the Lc subunit [9]. Furthermore, different fragmentation methods including higher energy collisional dissociation (HCD), hybrid ETD/HCD (EThcD), and 213-nm ultraviolet photodissociation (UVPD) have been applied for MDMS sequencing of mAbs [22]. Among them, during a single liquid chromatography (LC)-MS/MS run, EThcD and 213-nm UVPD provided 50 % and 60 % sequence coverage for Fc/2, respectively, but the sequence coverage of Fd was still less than 40 %. Recently, 193-nm UVPD realized about 80 % mAb sequence coverage by combining data from four LC-MS/MS runs [21].

This work introduces a novel multiple charge integration (MCI)-MDMS strategy coupled with UVPD for enhanced mAb sequencing. While conventional HCD and ETD fragmentation methods are significantly influenced by the charge state of mAb subunit ions, leading to variable fragmentation efficiency, 193-nm UVPD is relatively charge-independent in terms of fragmentation efficiency [24], resulting in different and complementary fragmentation patterns for protein ions with different charge states. Thus, integrating the UVPD spectra of mAb subunit ions with different charges could significantly improve the mAb sequence coverage. Based on this MCI-MDMS and UVPD strategy, near complete sequence coverage could be achieved for each mAb subunits, greatly facilitating the validation and sequencing of CDRs as well as the precise localization of post-translational modifications (PTMs) on mAb sequence (Fig. 1).

2. Experiment section

2.1. Materials and reagents

Deionized water used in all experiments was purified by Milli-Q system (Millipore Inc., Milford, Massachusetts, USA). Infliximab (Remicade) and cetuximab (Erbitux) were purchased from TopScience (Shanghai, China) with 98 % purity. IdeS protease was purchased from Yeasen Biotechnology (Shanghai, China). Neuraminidase and acetonitrile (ACN) were purchased from Merck (Darmstock, Germany). Other solvents were purchased from Sigma-Aldrich. All solvents and LC mobile phases were purchased with LC-MS grade purity. Micro Bio-Spin™ P-6 Gel columns purchased from Bio-Rad (California, USA). PLRP-S beads (1000 Å, 5 μm) was purchased from Agilent (California, USA).

2.2. Sample preparation

The antibody sample was dissolved in PBS (50 mM sodium phosphate, 150 mM NaCl, pH 6.6) at 5 μg/μl. Then, IdeS was added at 1 unit/μg of IgG, and two fragments of $F(ab')_2$ and Fc/2 were obtained by specifically cutting the hinge region for 30 min at 37 °C. After digestion, 6 M urea was added to denature these two fragments for 20 min. Then, 5 mM TCEP was added to open the disulfide bond to reduce $F(ab')_2$ into Lc and Fd fragments at room temperature for 30 min, followed by alkylation 30 min with 10 mM IAA in a dark environment. Micro Bio-Spin™ P-6 Gel columns were then used to exchange the buffer into 200 mM ammonium acetate. Cetuximab samples additionally were adjusted to pH 5 with 0.1 % formic acid (FA), and were treated with neuraminidase at 37 °C for 16 h to remove sialic acid. The cleaved mAb subunit samples were lyophilized and dissolved into 0.1 % FA aqueous solution at 1 μg/μL before analysis. The samples were prepared three times under the

same experimental conditions to ensure the reproducibility of the experiment.

2.3. LC-MS/MS analysis

The mAb subunit samples were loaded onto a 3 cm × 200 μm i.d. reversed phase (RP) trap column (PLRP-S, 1000 Å, 5 μm) and separated by a 15 cm × 75 μm i.d. PLRP-S separation column (1000 Å, 5 μm). The mobile phase A was 0.1 % FA and the mobile phase B was 0.1 % FA in 80 % ACN. The RP separation gradient was from 5 to 35 % mobile phase B in 5 min and from 35 to 60 % mobile phase B in 30 min with a flow rate of 300 nL/min. The LC was coupled with an Orbitrap Fusion Lumos Tribrid mass spectrometer (Thermo Fisher, San Jose, CA, USA) through a nano-electrospray ionization (nESI) source. A 193-nm ArF excimer laser (Gam laser, Orlando, FL, USA) was equipped for UVPD and MS/MS analysis as described in our previous report [25–27]. The temperature of the ion transfer capillary was 305 °C, the ESI voltage was 2000V, and the RF lens was set to 55 %. Before targeted MS analysis, the retention time and charge state distribution (CSD) of IgG subunits are pre-determined through a survey LC-MS/MS analysis. The MS1 full scan was set to a resolution of 15 K and a mass range of 400–2000 *m/z*. Then, targeted LC-MS/MS data was collected through selected ion monitor (SIM) mode. The MS/MS spectra were collected with a resolution of 240K. The AGC of MS/MS was set at 5E6 with maximum injection time of 500 ms. A 5-ns single pulse of laser irradiation was used for 193-nm UVPD analysis, with pulse energy varied within 0.6–1.4 mJ dependent on the CS of precursor ions. In SIM mode, hundreds of MS/MS spectra can be obtained continuously within the elution time of each mAb subunit. Averaging the spectra obtained from a single targeted LC-MS/MS analysis can greatly improve signal-to-noise ratio (S/N) and distribution of isotopic peaks. To compare with 193-nm UVPD, identical LC-MS/MS analysis was also performed using HCD with a normalized collision energy of 25 %.

2.4. Data analysis

The spectra of each antibody subunit acquired in a single LC-MS/MS were averaged and transformed to three individual raw files by FreeStyle (verison 1.5). The raw files were converted to mzML format by MSConvert [28] and then deconvolved using TopFD GUI (from TopPIC Suite, version 1.4.13) with a S/N of 10 [29]. The deconvoluted masses of UVPD fragment ions were firstly searched against a custom database including the monoisotopic masses of a, a+1, b, c, x, x+1, y, y-1, y-2, z and z+1 fragment ions with a mass tolerance of ±20 ppm using custom R scripts for estimating the averaged mass error [25]. Further, the deconvoluted masses of UVPD fragment ions were re-calibrated and subjected to a second round of matching with a mass tolerance of ±5 ppm. HCD spectra were processed similar as UVPD spectra but searched for b and y type product ions. In the ion matching process, alkylation (C_2H_3ON) was added to the Cys site at opened disulfide bond, and glycosylation (G0F, $C_{56}H_{92}O_{39}N_4$) was added to the Fc/2 subunit Asn61. For cetuximab, additional glutamine cyclization (Gln1, $-NH_3$) and glycosylation (Asn88, $C_{68}H_{112}O_{49}N_4$) were added to the Fd subunit for fragment ion matching. And the disulfide linkage between Cys131 and Cys189 of both infliximab and cetuximab was retained after treatment of TCEP and IAA [30], which was confirmed by MS1 and corresponding UVPD spectra. The disulfide linkage can be homolytic dissociated by UVPD [31]. Thus, the modifications of H loss at Cys131 and Cys189 were set to facilitate the assignment of fragment ions (Fig. S1).

3. Result and discussion

3.1. The development of MCI and UVPD strategy

We collected the MS/MS spectra of protein ions with specific charge state through SIM mode and averaged them to enhance S/N. Subsequently, the averaged UVPD spectra of protein ions with different charges were deconvoluted and integrated, facilitating the derivation of the protein sequence. At first, myoglobin (Mb) was utilized as a standard protein to demonstrate the efficiency of this MCI and UVPD strategy. The total ion chromatogram and CSD of Mb are shown in Fig. S2. Using targeted scanning in the SIM mode, we collected UVPD spectra of Mb ions with charge states from 16+ to 20+. Although the overall sequence coverages obtained by each run were comparable (about 80 %), different UVPD fragmentation patterns were observed at different charge states (Fig. S3A). Mb ions with different charge states have different conformations, resulting in different UVPD fragmentation pattern. Based on the heterogeneity of UVPD fragmentation patterns to

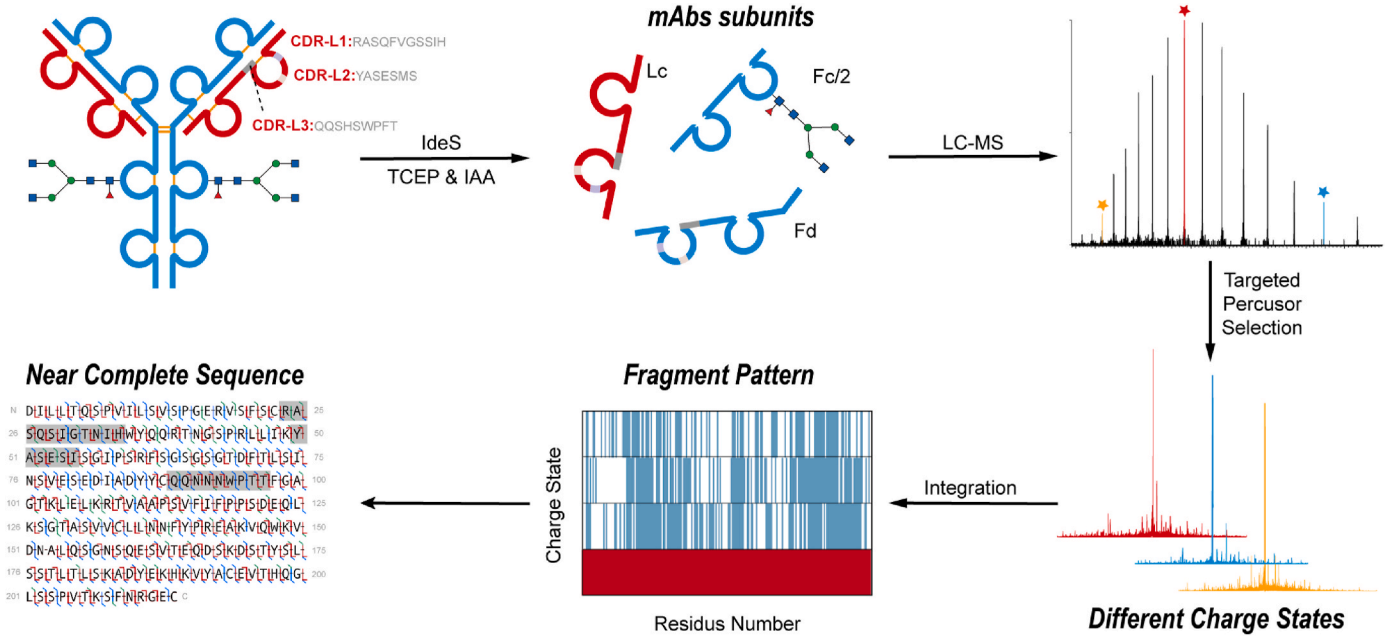

Fig. 1. The workflow schematics of multiple charge integration (MCI)-middle down mass spectrometry (MDMS) approach coupled with ultraviolet photodissociation (UVPD) and tandem MS (MS/MS) analysis for mAb sequencing.

charge states, the combination results of Mb ions with charge states 16+ to 18+ could improve the Mb sequence coverage to 92 %, which could not be simply achieved by repeat analysis of Mb ion with a single charge state (about 86 %, Figs. S3B–C). Overall, the combination of MCI and UVPD can greatly boost the sequence coverage of MS-based protein sequencing.

3.2. MCI-MDMS and UVPD strategy for infliximab sequencing

Then, the therapeutic IgG1 antibody infliximab was pre-cleaved to three subunits Fc/2, Fd, and Lc as described in experimental section. The separation of the three subunits of Infliximab is shown in Fig. S4A. A wide CSDs mainly from 16+ to 30+ were observed for the three subunits and the measured MWs were Fc/2, 25298.82 Da (G0F); Lc, 23707.78 Da; and Fd, 26029.12 Da (Figs. S5A–C). The SIM acquisition time corresponding to each subunit is shown in Table S1. In addition, two common PTMs including glycosylation and C-terminal lysine truncation were observed in the heavy chain (Fd and Fc/2) of infliximab with clear mass difference among different glycoforms (Fig. 2). The glycoforms identified at the C-terminus of infliximab heavy chain (Fc/2) were mainly G0, G0F, G1F, and G2F.

Then, targeted MS/MS fragmentation was performed on the different charge states of infliximab subunits. A narrow isolation window of 5 *m/z* was applied to avoid the interferences from adjacent peaks, which is especially critical for PTM localization [32]. Moreover, the UVPD pulse energy was optimized for subunit ions with different charge states. In general, protein ions with high charge state have more protonation sites and extended comformation, promoting more extensive cleavage during UVPD process [33]. Therefore, we adjusted the UVPD pulse energy from 1.4 to 0.6 mJ when the subunit charge state was increased from 16+ to 30+ to avoid over-fragmentation. An averaged sequence coverage of about 55 % could be obtained for a single charge subunit by UVPD, which is inferior to the results of Mb. This could be attributed to the higher MW and charge state of mAb subunits, leading to the unfavorable overlaps of the isotopic peaks in UVPD spectra.

The sequence coverage of infliximab subunits with different charge states are similar but exhibit different fragmentation patterns (Fig. 3C–E). Integrating the UVPD spectra of different charge states could improve the sequence cleavages to over 95 % for all the three subunits of infliximab. Near full sequence coverage greatly improves sequencing reliability and enables more accurate identification of CDR sites. For comparison, the Fc/2, Lc, and Fd of infliximab with specific charge states were also subjected to targeted MCI-MDMS and HCD analysis, resulting in inferior performance especially for sequencing the N-glycosylated Fc/2 (Fig. S6). HCD prefers to fragment glycans while leaves the protein backbone undissociated [34]. As a high energy and fast activation method, UVPD generates rich types of sequence-informative fragment ions, while minimizes the loss of unstable modifications [35]. About 270 fragments are assigned to sequence-matched ions in the averaged UVPD spectra, which is 6-folds of HCD. Further integrating the fragment ions obtained from Fc/2 (25+, 26+ and 27+), Lc (21+, 22+ and 23+), and Fd (24+, 25+ and 26+) subunits with 3 different charge states, the sequence coverages are improved from 25.8, 34.7, 32.4 % for HCD to about 76.1, 80.8, 74.4 % for UVPD, respectively, which greatly facilitated the sequencing and localization of N-glycosylated site (Fig. 3B). For CDRs, the results of UVPD are also significantly better than those of HCD. After integrating 3 charge states, HCD has only 0, 0, and 33.3 % sequence coverages for the three CDRs of Lc subunit, while UVPD has 40, 100, and 62.5 % sequence coverages. In CDRs of Fd subunit, HCD has sequence coverages of 50, 11.1, and 62.5 %, while UVPD has sequence coverages of 50, 88.9, and 87.5 %. Overall, the MCI-MDMS strategy is capable of therapeutic mAb sequencing with full coverage of all variable regions (Fig. 3C-E), which is much better than previous workflow based on specific charge state sequencing.

3.3. Cetuximab sequencing and MCI-MDMS strategy optimization

Cetuximab, different from other mAbs, contains an additional glycosylation site at the N-terminus of the heavy chain, showing

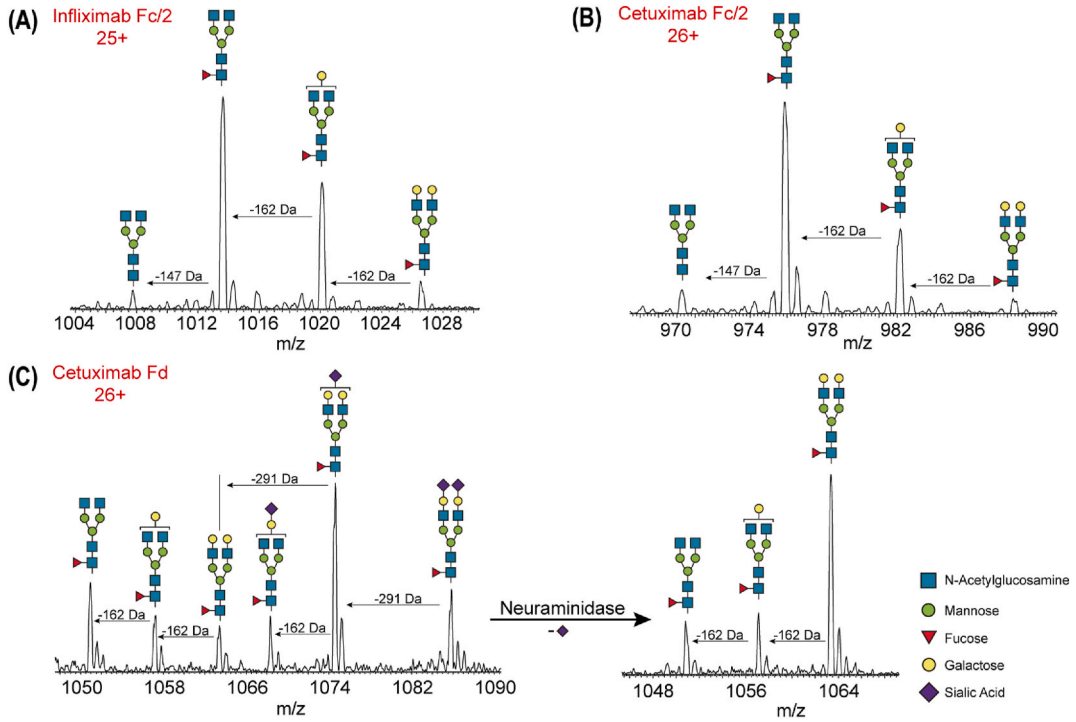

Fig. 2. The MS1 spectra of infliximab (A) and cetuximab (B) Fc/2 subunits with G0, G0F, G1F, and G2F glycoforms. The cetuximab Fd subunit showed abundant G2FS1 glycoforms due to the presence of sialic acid, and G2F, G1F and G0F glycoforms were mainly retained after sialic acid removal, among which the G2F abundance was greatly increased (C).

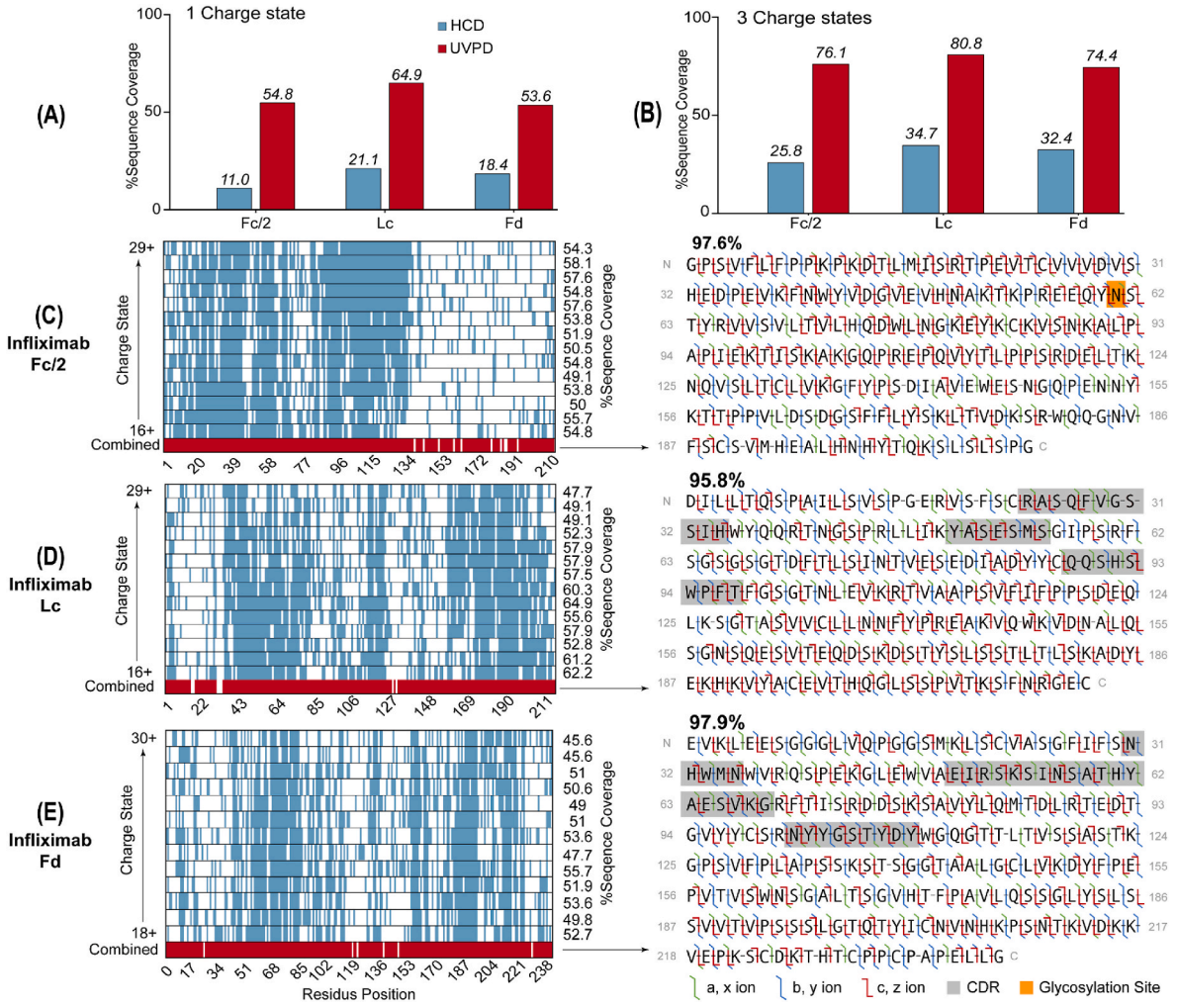

Fig. 3. Comparison of sequence coverages obtained by HCD and UVPD for 25+ of Fc/2, 21+ of Lc, and 24+ of Fd (A) and three charge state integration (B) in infliximab sequencing. The UVPD fragmentation patterns of all charge states of infliximab Fc/2 (C), Lc (D), and Fd (E), showing the cleavage sites and sequence coverage among different charge sates as well as the integrated sequence coverages. The CDRs are marked with a shaded part.

complicated glycoforms due to the existence of sialic acid [36]. Thus, neuraminidase [37] was pre-added to eliminate sialic acid during sample processing. The elution window and CSD of cetuximab were determined (Fig. S4B and Fig. S5D-E), and the MWs of cetuximab subunits were measured as Fc/2, 25330.55 Da (G0F); Lc, 23695.66 Da; and Fd, 27603.37 Da (G2F). Three PTMs located in the heavy chain were observed on cetuximab subunits Fd and Fc/2 including glycosylation, C-terminal lysine truncation, and N-terminal glutamine cyclization. The glycoforms identified in the Fc/2 fragment were similar to the infliximab Fc/2 fragment, while the glycosylation of the Fd fragment changed from G2FS2, G2FS1, G2F, G1F and G0F to G2F, G1F and G0F after desialylation, and the most abundant glycoforms was G2F (Fig. 2B and C). The UVPD spectra for all charge states of cetuximab subunit ions were collected and integrated, and over 95 % sequence coverages were also obtained for the three subunits (Fig. S7). Moreover, all six CDRs of cetuximab were completely sequenced by the MCI-MDMS and UVPD strategy, which was also much better than HCD.

Then, we sought to improve the sequencing throughput while retaining high sequence coverage by selectively integrating specific charge states with high complementarity in UVPD fragmentation patterns. In general, the subunit ions with adjacent charge states share conformation in gas phase, resulting in similar fragmentation patterns and low complementarity [38]. To maximize the utilization of this complementarity, all collected charge states were classified into three categories: low (16+ to 20+), medium (21+ to 25+), and high (26+ to 30+). Different combinations of these charge states were employed to achieve the highest possible sequence coverage. The results demonstrate that there is better fragment complementarity between charge states that are further apart, which is consistent with previous observations (Fig. S8). Therefore, a combination of three charge states—low, medium, and high—for each subunit was utilized to achieve optimal sequence coverage.

After optimizing, a sequence cleavage of nearly 90 % could be achieved for Lc subunit and nearly 80 % could be achieved for Fc/2 and Fd subunits of cetuximab with confident identification of CDR sites and PTM modifications, while reducing the overall analytical time by near 5-folds (Fig. 4). The complementarity of matched amino acid sites among the three charge states is summarized and the numbers of uniquely matched sites at each subunit accounts for 30 %–35 % of the total. These results emphasize the significance of using complementary charge states to achieve higher sequencing coverage and throughput.

4. Conclusion

In summary, we propose a novel UVPD based MCI-MDMS strategy for therapeutic mAb sequencing. By coupling this approach with 193-nm UVPD, we achieve nearly full sequence coverage of mAbs, particularly in the critical CDRs. Additionally, this method enables the confident identification and localization of PTM sites, including glycosylation, N-terminal glutamine cyclization, and C-terminal lysine truncation.

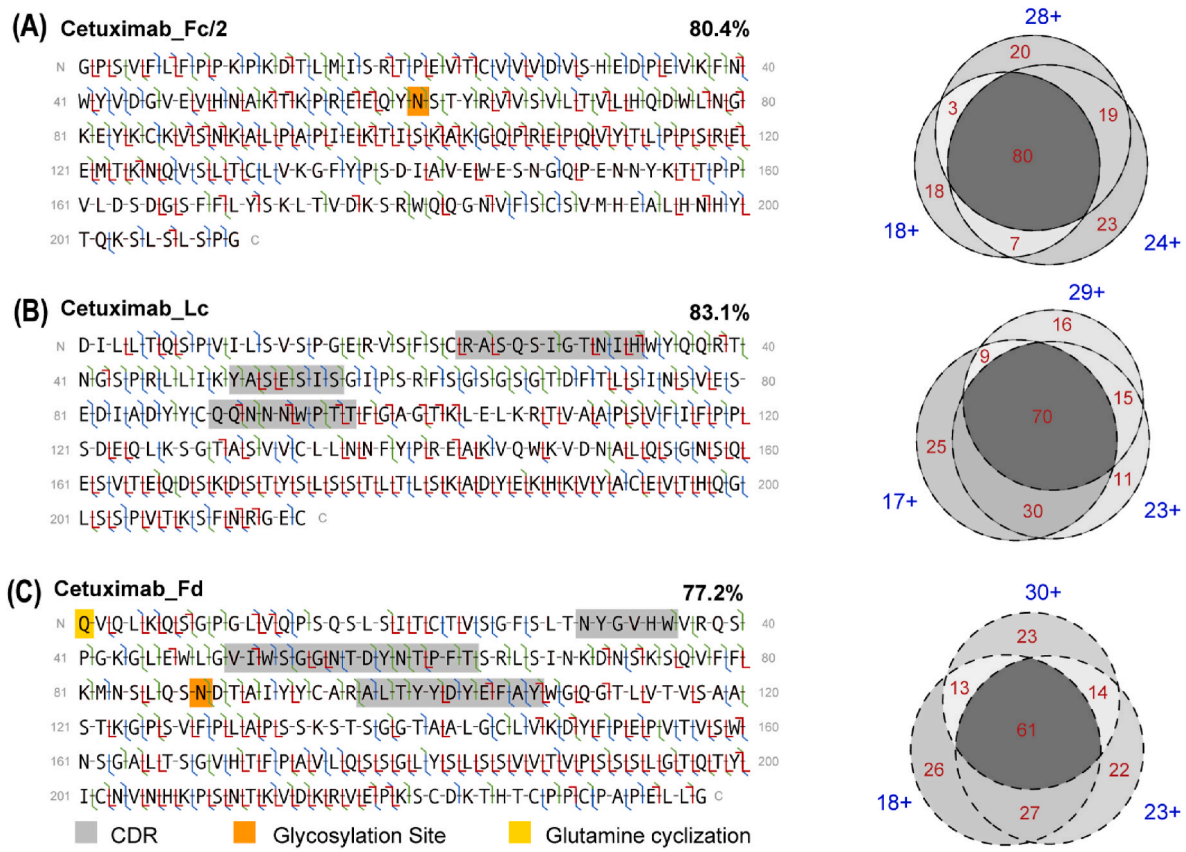

Fig. 4. UVPD fragmentation patterns of the three subunits of cetuximab integrated with low, medium, and high charge states. Fd fragment N-terminal glutamine cyclization, heavy chain N-terminal and C-terminal glycosylation, and CDRs have been highlighted in different colors. For each panel, the right side shows the corresponding Venn diagram of shared/unique matched amino acid sites for each of the three charge states. (For interpretation of the references to color in this figure legend, the reader is referred to the Web version of this article.)

Subsequently, by integrating different charge states with high UVPD fragmentation complementarity, we identify the optimal combination of low, medium, and high charge states. This integration further increases sequencing throughput while ensuring high sequence coverage. The combination of MCI-MDMS and UVPD represents a new and powerful method for mAb sequencing, realizing high sequence coverage and reliable PTM determination. This approach holds significant potential for the future sequencing of unknown mAbs, providing a crucial tool for the discovery and development of therapeutic mAbs.

CRediT authorship contribution statement

Jialiang Liu: Writing – review & editing, Writing – original draft, Resources, Methodology, Investigation, Data curation, Conceptualization. **Zheyi Liu:** Writing – review & editing, Software, Project administration, Methodology, Investigation, Data curation, Conceptualization. **Heng Zhao:** Methodology, Data curation. **Chunlei Xiao:** Supervision, Resources. **Xueming Yang:** Supervision, Resources. **Fangjun Wang:** Writing – review & editing, Supervision, Resources, Methodology, Funding acquisition, Data curation, Conceptualization.

Declaration of competing interest

The authors declare that they have no known competing financial interests or personal relationships that could have appeared to influence the work reported in this paper.

Acknowledgment

We acknowledged the financial supported by National Key R&D Program of China (2022YFA1304601), National Natural Science Foundation of China (32088101, 22288201, 92253304 and 22204165), and DICP (DICP I202242 and DICP I202228). The authors acknowledge the technological support of the biological mass spectrometry station of Dalian Coherent Light Source.

Appendix A. Supplementary data

Supplementary data to this article can be found online at https://doi.org/10.1016/j.aca.2024.343450.

Data availability

Data will be made available on request.

References

[1] J.K.H. Liu, The history of monoclonal antibody development - progress, remaining challenges and future innovations, Ann. Med. Surg. 3 (2014) 113–116, https://doi.org/10.1016/j.amsu.2014.09.001.
[2] A. Beck, T. Wurch, C. Bailly, N. Corvaia, Strategies and challenges for the next generation of therapeutic antibodies, Nat. Rev. Immunol. 10 (2010) 345–352, https://doi.org/10.1038/nri2747.
[3] A. Mullard, FDA approves 100th monoclonal antibody product, Nat. Rev. Drug Discov. 20 (2021) 491–495, https://doi.org/10.1038/d41573-021-00079-7.
[4] H. Kaplon, S. Crescioli, A. Chenoweth, J. Visweswaraiah, J.M. Reichert, Antibodies to watch in 2023, mAbs 15 (2023), https://doi.org/10.1080/19420862.2022.2153410.
[5] L.M. Weiner, J.C. Murray, C.W. Shuptrine, Antibody-based immunotherapy of cancer, Cell 148 (2012) 1081–1084, https://doi.org/10.1016/j.cell.2012.02.034.
[6] A.M. Scott, J.D. Wolchok, L.J. Old, Antibody therapy of cancer, Nat. Rev. Cancer 12 (2012) 278–287, https://doi.org/10.1038/nrc3236.

[7] J. Li, Z. Zhu, Research and development of next generation of antibody-based therapeutics, Acta Pharmacol. Sin. 31 (2010) 1198–1207, https://doi.org/10.1038/aps.2010.120.
[8] P. Sondermann, D.E. Szymkowski, Harnessing Fc receptor biology in the design of therapeutic antibodies, Curr. Opin. Immunol. 40 (2016) 78–87, https://doi.org/10.1016/j.coi.2016.03.005.
[9] L. Fornelli, D. Ayoub, K. Aizikov, A. Beck, Y.O. Tsybin, Middle-down analysis of monoclonal antibodies with electron transfer dissociation Orbitrap fourier transform mass spectrometry, Anal. Chem. 86 (2014) 3005–3012, https://doi.org/10.1021/ac4036857.
[10] C. Klein, U. Brinkmann, J.M. Reichert, R.E. Kontermann, The present and future of bispecific antibodies for cancer therapy, Nat. Rev. Drug Discov. 23 (2024) 301–319, https://doi.org/10.1038/s41573-024-00896-6.
[11] K. Tsuchikama, Y. Anami, S.Y.Y. Ha, C.M. Yamazaki, Exploring the next generation of antibody-drug conjugates, Nat. Rev. Clin. Oncol. 21 (2024) 203–223, https://doi.org/10.1038/s41571-023-00850-2.
[12] H.A. Alhazmi, M. Albratty, Analytical techniques for the characterization and quantification of monoclonal antibodies, Pharmaceuticals 16 (2023), https://doi.org/10.3390/ph16020291.
[13] A. Beck, E. Wagner-Rousset, D. Ayoub, A. Van Dorsselaer, S. Sanglier-Cianferani, Characterization of therapeutic antibodies and related products, Anal. Chem. 85 (2013) 715–736, https://doi.org/10.1021/ac3032355.
[14] M.-P. Lefranc, G. Lefranc, IMGT and 30 Years of immunoinformatics insight in antibody V and C domain structure and function, Antibodies 8 (2019) 29, https://doi.org/10.3390/antib8020029.
[15] D. Schulte, W. Peng, J. Snijder, Template-based assembly of proteomic short reads for de novo antibody sequencing and repertoire profiling, Anal. Chem. 9 (2022) 10391–10399, https://doi.org/10.1021/acs.analchem.2c01300.
[16] C.T. Watson, J. Glanville, W.A. Marasco, The individual and population genetics of antibody immunity, Trends Immunol. 38 (2017) 459–470, https://doi.org/10.1016/j.it.2017.04.003.
[17] W. Peng, M.F. Pronker, J. Snijder, Mass spectrometry-based de novo sequencing of monoclonal antibodies using multiple proteases and a dual fragmentation scheme, J. Proteome Res. 20 (2021) 3559–3566, https://doi.org/10.1021/acs.jproteome.1c00169.
[18] S.C. de Graaf, M. Hoek, S. Tamara, A.J.R. Heck, A perspective toward mass spectrometry-based de novo sequencing of endogenous antibodies, mAbs 14 (2022), https://doi.org/10.1080/19420862.2022.2079449.
[19] K. Srzentić, L. Fornelli, Y.O. Tsybin, J.A. Loo, H. Seckler, J.N. Agar, L.C. Anderson, D.L. Bai, A. Beck, J.S. Brodbelt, Y.E.M. van der Burgt, J. Chamot-Rooke, S. Chatterjee, Y. Chen, D.J. Clarke, P.O. Danis, J.K. Diedrich, R.A. D'Ippolito, M. Dupré, N. Gasilova, Y. Ge, Y.A. Goo, D.R. Goodlett, S. Greer, K.F. Haselmann, L. He, C.L. Hendrickson, J.D. Hinkle, M.V. Holt, S. Hughes, D.F. Hunt, N. L. Kelleher, A.N. Kozhinov, Z. Lin, C. Malosse, A.G. Marshall, L. Menin, R. J. Millikin, K.O. Nagornov, S. Nicolardi, L. Paša-Tolić, S. Pengelley, N. R. Quebbemann, A. Resemann, W. Sandoval, R. Sarin, N.D. Schmitt, J. Shabanowitz, J.B. Shaw, M.R. Shortreed, L.M. Smith, F. Sobott, D. Suckau, T. Toby, C.R. Weisbrod, N.C. Wildburger, J.R. Yates 3rd, S.H. Yoon, N.L. Young, M. Zhou, Interlaboratory study for characterizing monoclonal antibodies by top-down and middle-down mass spectrometry, J. Am. Soc. Mass Spectrom. 31 (2020) 1783–1802, https://doi.org/10.1021/jasms.0c00036.
[20] J.B. Shaw, W. Liu, Y.V. Vasil'ev, C.C. Bracken, N. Malhan, A. Guthals, J. S. Beckman, V.G. Voinoy, Direct determination of antibody chain pairing by top-down and middle-down mass spectrometry using electron capture dissociation and ultraviolet photodissociation, Anal. Chem. 92 (2020) 766–773, https://doi.org/10.1021/acs.analchem.9b03129.
[21] V.C. Cotham, J.S. Brodbelt, Characterization of therapeutic monoclonal antibodies at the subunit-level using middle-down 193 nm ultraviolet photodissociation, Anal. Chem. 88 (2016) 4004–4013, https://doi.org/10.1021/acs.analchem.6b00302.
[22] L. Fornelli, K. Srzentic, R. Huguet, C. Mullen, S. Sharma, V. Zabrouskov, R. T. Fellers, K.R. Durbin, P.D. Compton, N.L. Kelleher, Accurate sequence analysis of a monoclonal antibody by top-down and middle-down Orbitrap mass spectrometry applying multiple ion activation techniques, Anal. Chem. 90 (2018) 8421–8429, https://doi.org/10.1021/acs.analchem.8b00984.
[23] J. Sjogren, F. Olsson, A. Beck, Rapid and improved characterization of therapeutic antibodies and antibody related products using IdeS digestion and subunit analysis, Analyst 141 (2016) 3114–3125, https://doi.org/10.1039/c6an00071a.
[24] A. Bashyal, J.D. Sanders, D.D. Holden, J.S. Brodbelt, Top-down analysis of proteins in low charge states, J. Am. Soc. Mass Spectrom. 30 (2019) 704–717, https://doi.org/10.1007/s13361-019-02146-1.
[25] L. Zhou, Z. Liu, Y. Guo, S. Liu, H. Zhao, S. Zhao, C. Xiao, S. Feng, X. Yang, F. Wang, Ultraviolet photodissociation reveals the molecular mechanism of crown ether microsolvation effect on the gas-phase native-like protein structure, J. Am. Chem. Soc. 145 (2023) 1285–1291, https://doi.org/10.1021/jacs.2c11210.
[26] Z. Liu, Z. Qin, C. Cui, et al., In-situ generation and global property profiling of metal nanoclusters by ultraviolet laser dissociation-mass spectrometry, Sci. China Chem. 65 (2022) 1196–1203, https://doi.org/10.1007/s11426-022-1267-5.
[27] Binwen Sun, Zheyi Liu, Fang Xiang, Xiaolei Wang, Can Lai, Lin Liu, Chunlei Xiao, You Jiang, Fangjun Wang, Improving the performance of proteomic analysis via VAILase cleavage and 193-nm ultraviolet photodissociation, Anal. Chim. Acta 1155 (2021) 338–340, https://doi.org/10.1016/j.aca.2021.338340.
[28] M.C. Chambers, B. Maclean, R. Burke, D. Amodei, D.L. Ruderman, S. Neumann, L. Gatto, B. Fischer, B. Pratt, J. Egertson, K. Hoff, D. Kessner, N. Tasman, N. Shulman, B. Frewen, T.A. Baker, M.-Y. Brusniak, C. Paulse, D. Creasy, L. Flashner, K. Kani, C. Moulding, S.L. Seymour, L.M. Nuwaysir, B. Lefebvre, F. Kuhlmann, J. Roark, P. Rainer, S. Detlev, T. Hemenway, A. Huhmer, J. Langridge, B. Connolly, T. Chadick, K. Holly, J. Eckels, E.W. Deutsch, R. L. Moritz, J.E. Katz, D.B. Agus, M. MacCoss, D.L. Tabb, P. Mallick, A cross-platform toolkit for mass spectrometry and proteomics, Nat. Biotechnol. 30 (2012) 918–920, https://doi.org/10.1038/nbt.2377.
[29] Q. Kou, L. Xun, X. Liu, TopPIC: a software tool for top-down mass spectrometry-based proteoform identification and characterization, Bioinformatics 32 (2016) 3495–3497, https://doi.org/10.1093/bioinformatics/btw398.
[30] M.-C. Sun, C.-D. Chen, Y.-S. Huang, Z.-S. Wu, Y.-P. Ho, Matrix-assisted laser desorption/ionization-MS-based relative quantification of peptides and proteins using iodoacetamide and N-methyliodoacetamide as labeling reagents, J. Separ. Sci. 31 (2008) 538–547, https://doi.org/10.1002/jssc.200700440.
[31] M.M. Quick, C.M. Crittenden, J.A. Rosenberg, J.S. Brodbelt, Characterization of disulfide linkages in proteins by 193 nm ultraviolet photodissociation (UVPD) mass spectrometry, Anal. Chem. 90 (2018) 8523–8530, https://doi.org/10.1021/acs.analchem.8b01556.
[32] J. Dhenin, M. Dupre, K. Druart, A. Krick, C. Mauriac, J. Chamot-Rooke, A multiparameter optimization in middle-down analysis of monoclonal antibodies by LC-MS/MS, J. Mass Spectrom. 58 (2023), https://doi.org/10.1002/jms.4909.
[33] Z. Hall, C.V. Robinson, Do charge state signatures guarantee protein conformations? J. Am. Soc. Mass Spectrom. 23 (2012) 1161–1168, https://doi.org/10.1007/s13361-012-0393-z.
[34] S.M. Greer, J.S. Brodbelt, Top-down characterization of heavily modified histones using 193 nm ultraviolet photodissociation mass spectrometry, J. Proteome Res. 17 (2018) 1138–1145, https://doi.org/10.1021/acs.jproteome.7b00801.
[35] J.S. Brodbelt, L.J. Morrison, I. Santos, Ultraviolet photodissociation mass spectrometry for analysis of biological molecules, Chem. Rev. 120 (2020) 3328–3380, https://doi.org/10.1021/acs.chemrev.9b00440.
[36] D. Ayoub, W. Jabs, A. Resemann, W. Evers, C. Evans, L. Main, C. Baessmann, E. Wagner-Rousset, D. Suckau, A. Beck, Correct primary structure assessment and extensive glyco-profiling of cetuximab by a combination of intact, middle-up, middle-down and bottom-up ESI and MALDI mass spectrometry techniques, mAbs 5 (2013) 699–710, https://doi.org/10.4161/mabs.25423.
[37] S. Rosati, Y. Yang, A. Barendregt, A.J.R. Heck, Detailed mass analysis of structural heterogeneity in monoclonal antibodies using native mass spectrometry, Nat. Protoc. 9 (2014) 967–976, https://doi.org/10.1038/nprot.2014.057.
[38] Y. Mao, M.A. Ratner, M.F. Jarrold, Molecular dynamics simulations of the charge-induced unfolding and refolding of unsolvated cytochrome, J. Phys. Chem. B 103 (1999) 10017–10021, https://doi.org/10.1021/jp991093d.